

DOI: 10.1002/adfm.200701208

Embedded Shape-Memory Alloy Wires for Improved Performance of Self-Healing Polymers**

By Eva L. Kirkby, Joseph D. Rule, Véronique J. Michaud, Nancy R. Sottos, Scott R. White, and Jan-Anders E. Månson*

We report the first measurements of self-healing polymers with embedded shape-memory alloy (SMA) wires. The addition of SMA wires shows improvements of healed peak fracture loads by up to a factor of 1.6, approaching the performance of the virgin material. Moreover, the repairs can be achieved with reduced amounts of healing agent. The improvements in performance are due to two main effects: (i) crack closure, which reduces the total crack volume and increases the crack fill factor for a given amount of healing agent and (ii) heating of the healing agent during polymerization, which increases the degree of cure of the polymerized healing agent.

1. Introduction

A distinctive physical characteristic of living materials is their ability to detect mechanical damage—such as a skin abrasion or bone fracture—and to heal themselves. Recent advances in composite materials have made the first steps to replicate the self-healing properties of living materials. Such materials should be especially valuable in applications where it is impractical or impossible to repair the material when it is in use, such as in the aerospace or sports industries. Both solid-state and liquid-state healing approaches are being developed; this paper focuses on liquid-based methods. The basic concept is to embed both a liquid monomer and a hardener in the epoxy matrix, and to bring them into contact at the time and site of the injury to effect the repair.^[1,2]

White and coworkers store the liquid healing agent (dicyclopentadiene (DCPD)) in microcapsules, and the solid catalyst (Grubbs' catalyst) in wax particles.^[3] Upon damage, a crack propagates through the material and ruptures the microcapsules along the fracture plane. Subsequently, the low-viscosity healing agent is released and covers the crack plane by capillary action. On contact with the catalyst, ring

opening metathesis polymerization (ROMP) occurs and the crack is healed at ambient temperature. Similarly, Yin et al. have used $\text{CuBr}_2(2\text{-MeIm})_4$ latent hardener dispersed in an epoxy matrix to cure epoxy released from microcapsules at the time of damage, by thermal activation at 130 °C for 1 h.^[4] Microcapsules of the appropriate size and shell-wall thickness are robust and do not rupture easily during manufacture. Moreover, they toughen the matrix by a combination of crack-pinning and localized plastic deformation.^[5]

Another approach is being developed by Trask et al., using hollow glass fibers infused with either healing or curing agent (Cycom 823 two-part system).^[6–8] These fibers are placed at critical damage interfaces in a carbon or glass fiber composite. When the composite is impacted, the healing fibers rupture, releasing the healing agent into the damage zone. Although this technique appears capable of restoring the full strength of the undamaged composite, the healing fibers cause an intrinsic reduction in flexural strength (around 10–20%) compared with the standard composite. Moreover, the damage event drains the healing agent and catalyst from an area considerably larger than the damaged region alone, rendering an excessive area inactive for following repairs.

A third approach is being pursued by Toohey et al. in which a bio-inspired embedded vascular network is used to store and deliver the healing agent(s).^[9] To create this architecture, a three-dimensional microvascular network is embedded in the polymer substrate via direct-write assembly of a fugitive organic ink. Periodic three-dimensional scaffolds are first created by depositing the ink in a layer-by-layer build sequence followed by infiltration with an epoxy resin. The resin is then cured and the fugitive ink is subsequently removed under light vacuum by heating the structure to modest temperatures to liquefy the ink. Repeated healing of up to seven fracture–heal cycles was demonstrated in epoxy using the ROMP-based healing chemistry previously demonstrated in ref. [1].

[*] Prof. J.-A. E. Månson, E. L. Kirkby, Dr. V. J. Michaud
Laboratoire de Technologie des Composites et Polymères, Institut
des Matériaux
CH-1015 Lausanne (Switzerland)
E-mail: jan-anders.manson@epfl.ch

Dr. J. D. Rule, Prof. N. R. Sottos, Prof. S. R. White
Autonomic Materials Systems Group, Beckman Institute for
Advanced Science and Technology
University of Illinois at Urbana-Champaign
Urbana, IL 61801 (USA)

[**] The authors gratefully acknowledge the financial support of the Swiss National Science Foundation (contract no. 200020-1-5169) and of AFOSR Aerospace and Material Science Directorate (grant no. FA9550-05-1-0346). The authors thank Andrew Phillips for technical support and discussions.

In previous studies the typical microcapsule diameter was 100–200 μm , and their loading in the matrix about 10–20 wt%. There is significant interest to reduce the capsule size and concentration even further. Firstly, the smallest cracks that can be repaired are set by the microcapsule size; further reductions would allow the repair of progressively smaller microcracks. Furthermore, smaller microcapsules are necessary in materials where the characteristic dimensions are below 100 μm , such as thin coatings or high fiber-loaded composites. Finally, smaller microcapsule sizes and concentrations will allow for better processing — such as improved dispersion within the matrix — as well as reducing their influence on the properties of the original material. However, Rule et al. have found that the healed fracture toughness falls off substantially at low microcapsule sizes and concentrations due to the failure to completely fill the crack volume with healing agent.^[10] A technique is therefore required to reduce the crack size during the healing period, to allow the entire crack to be filled with a small volume of healing agent.

Shape-memory alloy (SMA) wires are well-suited to this application. They exhibit a thermoelastic martensitic phase transformation, contracting above their transformation temperature and exerting large recovery stresses of up to 800 MPa when constrained at both ends.^[11–13] Moreover, these large stresses are exerted over a large strain range of several percent. Rogers et al. have shown that, when an SMA wire is embedded within an epoxy matrix, the full recovery force acts at the free edges of the component.^[14] Therefore, an SMA wire bridging a crack should induce a large closure force on the crack. In this paper, we report the first study of combining SMA wires with a self-healing polymer, and investigate their influence on the self-healing properties.

2. Previous Results (Without SMA Wires)

Rule et al. studied the influence of microcapsule size and concentration on the self-healing properties of samples identical to the ones used in this study, but without any SMA wires.^[10] They performed tests with three different microcapsule diameters — 65, 151, and 386 μm — as well as a control where a known amount of DCPD was manually injected into the crack. They found that the healed peak load for all samples followed the same general curve (Fig. 1), which depends only on the amount of DCPD delivered per unit crack area, D_h (g cm^{-2}), given by,

$$D_h = \rho_s \phi d_c \quad (1)$$

where ρ_s is the density of the matrix (1.16 g cm^{-3}), ϕ the weight fraction of microcapsules, and d_c (cm) is the diameter of the microcapsules. The healed peak load (Fig. 1) shows two main characteristics. Firstly, a plateau of about 38 N is achieved at large values of delivered DCPD, corresponding to a healing efficiency of around 50% compared to the virgin

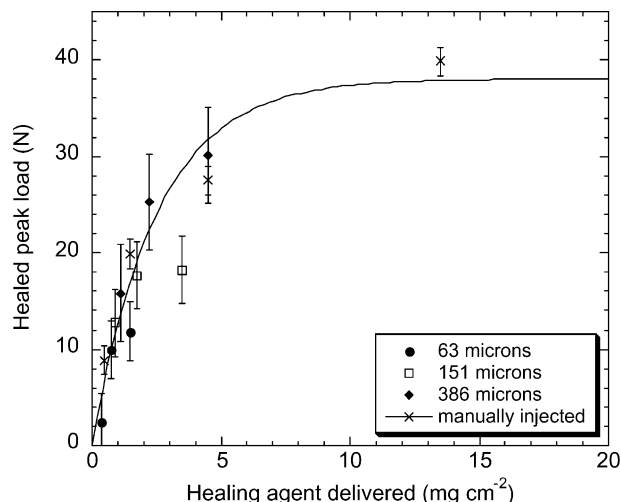


Figure 1. The average peak force required to fracture healed TDCB samples without SMA wires [10]. Tests were performed with various microcapsule sizes and concentrations, and also where the DCPD was manually injected into the crack. All data can be fitted with a universal curve (solid line) which depends only on the amount of DCPD delivered per unit crack area.

material. Secondly, at lower values of delivered DCPD, below 5 mg cm^{-2} , the healed peak load rapidly decreases. The onset of this reduced performance was found to occur when the total crack volume exceeded the volume of delivered healing agent, resulting in only partial coverage of the crack faces.

3. Results and Discussion

3.1. Effect of SMA Wires on Virgin Fracture Toughness

Experiments were carried out to determine if incorporating the SMA wires significantly altered the virgin matrix toughness. Tapered double cantilever beam (TDCB) samples were prepared as described in Section 5. The averaged virgin peak loads and their corresponding fracture toughness (Eq. 3) are summarized in Table 1. Both sets of data, with and without SMA wires, are consistent within the measurement errors. Thus, any improved self-healing performance reported here is due to improved healing of the crack, as opposed to a toughening effect of the embedded SMA wires.

Table 1. Effect of SMA wire presence on matrix fracture properties. The values without SMA wires were obtained by Rule et al.^[10]

Sample	With SMA wires		Without SMA wires	
	Virgin peak load [N]	K_{IC} [$\text{MPa m}^{1/2}$]	Virgin peak load [N]	K_{IC} [$\text{MPa m}^{1/2}$]
Epoxy	68.6	0.77 ± 0.10	77.7	0.87 ± 0.12
Epoxy/Grubbs' (5 wt.%)	78.5	0.88 ± 0.14	78.5	0.88 ± 0.10

3.2. Optical Measurements of Crack Closure

The crack face separation was measured by optical microscopy for several TDCB samples containing SMA wires, both before and after activation. An example image is shown in Figure 2. The cracks were imaged with an Olympus BX61 optical microscope, and the crack separation evaluated using the *analySIS Image Processing* program. The crack opening was calculated as the average of three measurements taken at different locations along its length. Two sets of samples were made: the first consisted of epoxy with SMA wires, and the second of epoxy and localized wax-protected Grubbs' catalyst microspheres ($360 \pm 40 \mu\text{m}$ diameter) with SMA wires.

The samples were fractured in the standard fashion, and the crack opening was measured at each of the three wire locations. The average of the three measurements was taken for each sample, giving an average crack opening of $160 \pm 35 \mu\text{m}$ (range: $80\text{--}300 \mu\text{m}$) before SMA activation. The SMA wires were then activated, and the crack opening re-measured at the same three locations. These measurements were repeated on four samples without catalyst microspheres and four samples with catalyst microspheres. Once the SMA wires were activated, the average crack opening was $15 \pm 3 \mu\text{m}$ (range: $8\text{--}23 \mu\text{m}$) for samples without catalyst, and $18 \pm 4 \mu\text{m}$ (range: $3\text{--}35 \mu\text{m}$) for samples with catalyst. Activation of the embedded SMA wires reduces the crack face separation by about an order of magnitude. After SMA activation, the crack volumes were 1.8 and $2.1 \mu\text{L}$ for the samples without and with Grubbs' catalyst, respectively. The reduction in crack volume suggests that full healing can be

achieved with relatively small volumes of DCPD healing agent (around 2 mg cm^{-2} , c.f. Fig. 1).

3.3. Healing with SMA Wires and Injected Healing Agent

3.3.1. Healing Performance

For these tests the TDCB samples included wax-protected Grubbs' catalyst microspheres of $300 \pm 30 \mu\text{m}$ diameter. A typical test result is shown in Figure 3. In the virgin test the pre-crack advances slightly at about $700 \mu\text{m}$ displacement and 80 N load. The crack propagated unstably at about $850 \mu\text{m}$ displacement and 85 N load, before arresting at an SMA wire. Continued loading leads to a final rapid propagation of the crack through the entire sample at about $1170 \mu\text{m}$ displacement and 65 N load. After the virgin test, $20 \mu\text{L}$ of DCPD healing agent were injected into the crack. The SMA wires were then activated as described previously, and the sample allowed to heal for 24 h. They were then carefully debonded and removed from the matrix by hand. Upon re-testing, the sample had recovered a large fraction—about 98%—of the virgin load-bearing capacity.

This procedure was repeated for a series of samples involving 0, 1, 2, 5, 10, 14, and $20 \mu\text{L}$ of injected DCPD. The averaged healed peak loads are shown in Figure 4, together with the fit to the Rule et al. measurements for room temperature healing without SMA wires (Fig. 1). A clear improvement in healed peak load results when SMA wires are present; the healed peak loads are increased by about a factor

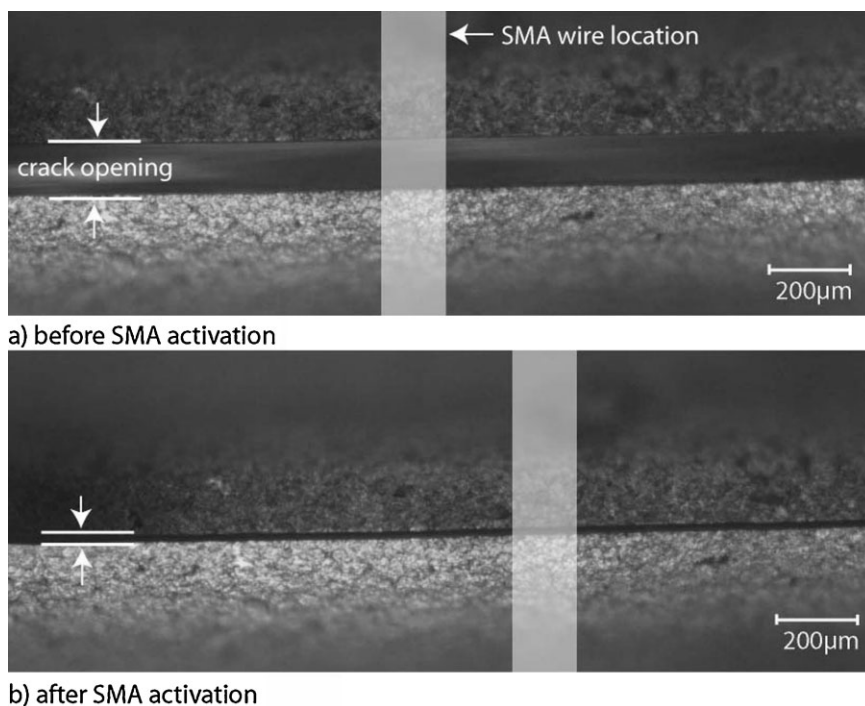


Figure 2. Optical microscope images of the crack in an epoxy/SMA TDCB sample, a) before the SMA wires were activated and b) after the SMA wires were activated. The crack opening at this location was reduced from $120 \mu\text{m}$ to about $17 \mu\text{m}$.

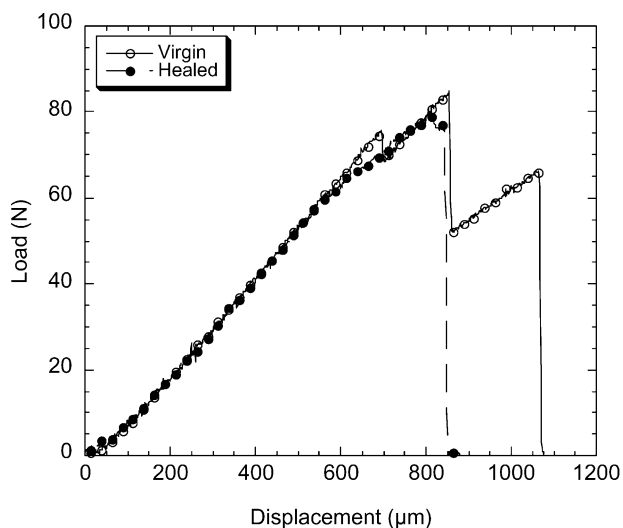


Figure 3. Example TDCB fracture test result for a sample with injected healing agent. The virgin sample was loaded in mode I to failure, and then removed from the load frame. After injecting 20 μL of DCPD, the SMA wires were activated for 30 min. The sample then healed at room temperature for a further 24 h, after which it was re-tested to failure. For this sample, about 98% of the virgin peak load was restored.

of 1.6 relative to the samples without SMA wires. Moreover, a dramatic improvement is achieved for the smallest quantities of healing agent delivered (1 and 2 μL), as was anticipated from the reduced crack opening measurements.

Representative virgin and healed load-displacement curves for samples with a fill factor well above unity, both with and without SMA wires, are compared in Figure 5. Consistent with results reported in ref. [3], the sample healed without SMA wires—at room temperature—exhibits a non-linear stress–

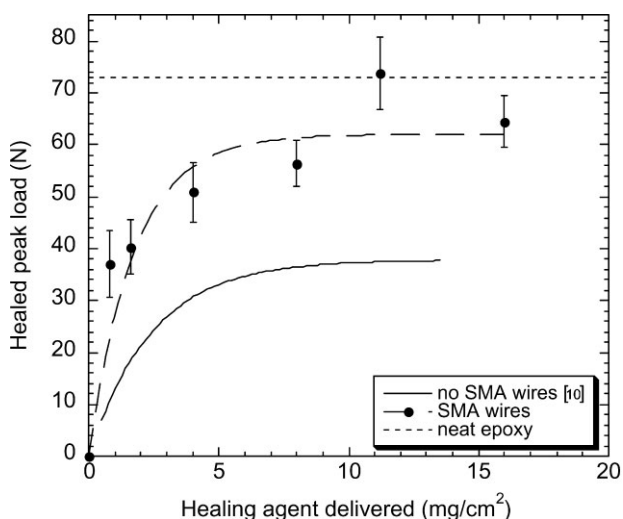


Figure 4. Summary of the healed peak loads of samples with injected healing agent (each data point represents the average of 4–10 identically prepared samples). The circles denote average values for samples healed with embedded SMA wires. The wires were activated for 30 min following injection of the healing agent and then healing occurred for an additional 24 h at room temperature. The solid curve is taken from Figure 1 (no SMA wires and 24 h room temperature healing).

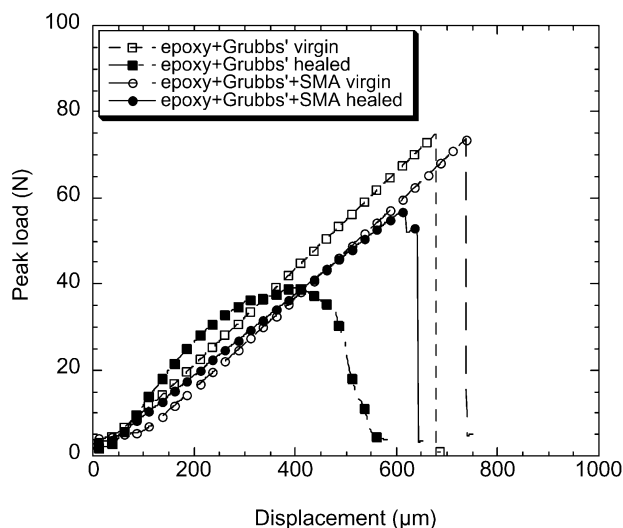


Figure 5. Typical healed load-displacement curves for TDCB samples, both with and without embedded SMA wires.

strain behavior. This non-linearity was attributed to a plasticization of the polyDCPD film by the dissolved wax.^[3] However, the samples healed with SMA wires—at elevated temperature—show linear behavior, similar to the virgin measurements (Fig. 5). The raised temperature in the SMA samples increases the rate and extent of dissolution of the wax, which in turn leads to a higher degree of polymerization of the DCPD than at room temperature, producing a film with superior mechanical and adhesive properties. This is supported with scanning electron images of the fracture surfaces of samples healed without and with SMA wires, Figure 6 and 7, respectively. In the case of the sample healed at room temperature (Fig. 6) the polyDCPD film appears flaky, and has become disconnected from the epoxy matrix in many locations. In contrast, the polyDCPD film in the sample healed with SMA wires (Fig. 7) is more continuous, and remains well-adhered to the fracture plane.

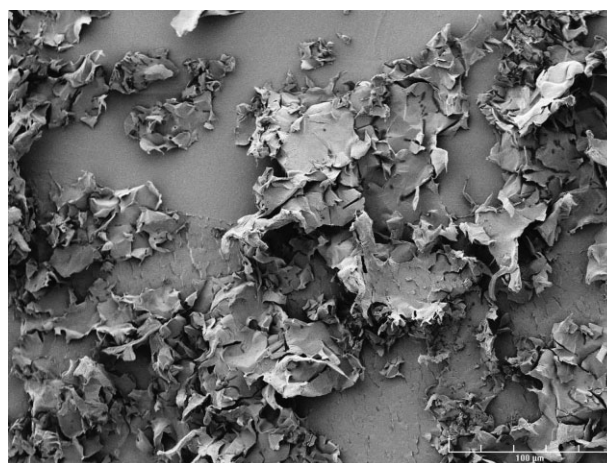


Figure 6. SEM image of a fracture surface of a TDCB sample healed at room temperature, without SMA wires.

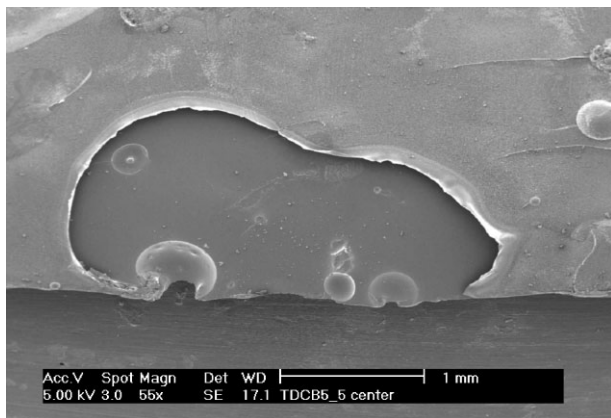


Figure 7. SEM image of a fracture surface of a TDCB sample healed with SMA wires.

3.3.2. Effect of Crack Volume

The healing efficiency is expected to depend not only on the amount of healing agent delivered, but also on the total volume of the closed crack, which shows considerable variability from sample to sample. Thus, we define the *fill factor* (γ) as the volume of injected healing agent divided by the healed total crack volume, i.e.,

$$\gamma = \frac{V_{\text{DCPD}}}{V_{\text{crack}}} \quad (2)$$

The crack opening, and hence volume, was measured using optical microscopy. (Some of the data in Fig. 4 cannot be re-plotted versus fill factor since the crack opening is unknown). In Figure 8, the individual data for 1, 2, 5, and 10 μL of DCPD injected are plotted versus the calculated fill factors. Notwithstanding the large sample-to-sample variations, the healed peak load for all injection volumes show qualitatively similar behavior, namely a plateau of the healed peak load around 50–60 N above a fill factor of unity. The 1 μL data do not reach complete fill and so do not show this plateau. The combined data for all cases are shown in Figure 9. The general trend of increasing healed peak load up to a fill factor of unity is consistent across all the data.

3.3.3. Factors Contributing to the Improved Performance for SMA Samples

The results clearly indicate that improved self-healing performance is obtained with the addition of SMA wires and their activation during healing. Two main factors can be identified that lead to this improved performance. Firstly, activation of the SMA wires leads to a large reduction in total crack

volume and a corresponding increase in the fill factor (γ). In this case improvements in healed peak load could be expected for cases where $\gamma \leq 1$ without activation. Secondly, activation of the SMA wires by resistive heating raises the local temperature of the matrix and the healing agent in the crack. In this case the healed material in the crack may be more completely cured, with superior mechanical and adhesive properties.

To elucidate the relative impact of each of these factors separately we performed two further tests. In the first we have isolated the effect of reduced crack volume by preparing TDCB samples identical to those used previously, but without SMA wires. These samples were fractured and subsequently 2 or 5 μL of DCPD were injected into the crack, the sample halves were brought back together, registered as closely as possible and then compressed using elastic bands to hold the crack plane closed. The samples were allowed to cure for 24 h at room temperature. After healing, crack openings were all below 10 μm , and the corresponding fill factors were all well above unity. Healed peak loads for these samples are shown in Figure 10, and averaged $36.8 \pm 1.7 \text{ N}$ for the 2 μL samples and $37.9 \pm 2.1 \text{ N}$ for the 5 μL samples. In comparison, Rule et al. obtained healed peak loads of $\sim 18.5 \pm 5$ and $\sim 30 \pm 5 \text{ N}$, respectively, for identical samples in which no closure force was applied (Fig. 1) (For this sample geometry, 1 μL of injected DCPD corresponds to 0.8 mg cm^{-2} delivered to the crack plane.).^[10]

In another set of experiments we isolated the effect of heating by preparing a set of TDCB samples in which the three SMA wires were replaced with three 200 μm diameter constantan wires, a non-shape-memory copper-nickel based

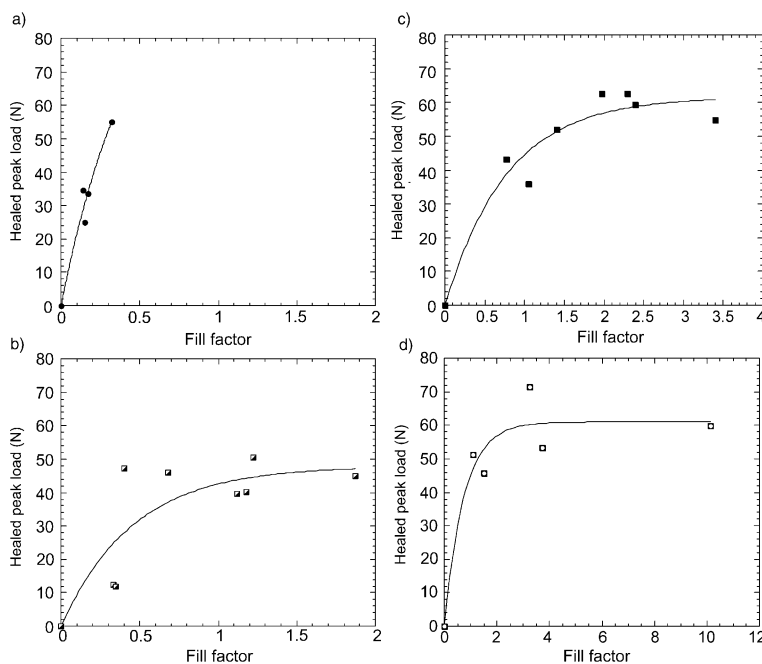


Figure 8. Healed peak load versus fill factor for TDCB samples injected with a) 1 μL , b) 2 μL , c) 5 μL , and d) 10 μL of DCPD. Each point represents a single measurement.

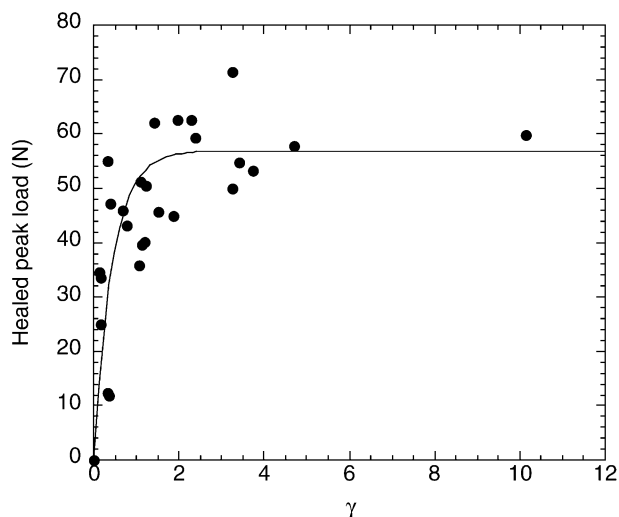


Figure 9. Healed peak load versus fill factor for all SMA samples combined.

alloy wire control. After virgin fracture, 2, 5, 15, or 20 μL of DCPD were injected into the crack and the sample halves were brought back together by hand. The constantan wires were free to slip through the matrix as the crack faces were brought back into contact, due to a thin layer of conducting paste on their surface. The constantan wires were then heated resistively for 30 min, to simulate the heat produced by the activated SMA wires. The SMA wires and the constantan wires have a resistance of 56.6 and 15.6 $\Omega\text{ m}^{-1}$, respectively. As a result, the constantan wires were heated with 0.95 A per wire for 30 min, so that the power dissipated in the two cases was the same.

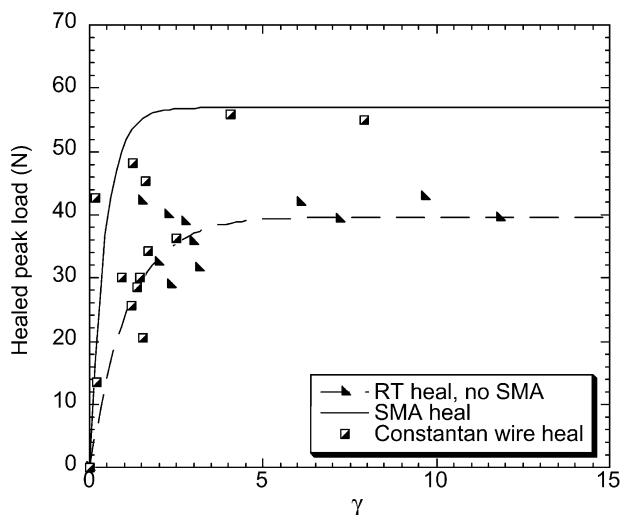


Figure 10. Healed peak load versus fill factor for samples a) without SMA wires, healed at room temperature and held together with a rubber band, b) with 200 μm diameter constantan wires, healed with the same heating cycle for the SMA wires, and c) with SMA wires, healed in the standard fashion described in Section 5.

After this 30 min period the samples were allowed to heal at room temperature for a further 24 h. The measurements for these tests are also shown in Figure 10, together with the curve for all SMA-healed samples from Figure 9. The constantan-healed samples with a low fill factor had a maximum healed peak load of around 30 N. However, as the fill factor increased, the healed peak loads of the constantan-healed samples reached the 60 N plateau value exhibited by the SMA-healed samples. This is consistent with expectations, namely that provided the fill factor is above unity, heating the samples improves the healed peak loads, by increasing the degree of cure of the DCPD healing agent.

These measurements are consistent with observations by Kessler et al., who measured the effect of temperature on the healed interlaminar fracture toughness in a delaminated self-healing structural composite.^[15] They prepared composite samples with the same EPON 828/DETA matrix used in this study, and plain-weave carbon fiber reinforcement. The samples were cured at room temperature for 24 h and post-cured at 30 $^{\circ}\text{C}$ for 48 h. They were then pin-loaded in tension and their interlaminar fracture toughness was determined. The samples were then allowed to heal for 48 h, either at room temperature or at 80 $^{\circ}\text{C}$, and re-tested. Room temperature samples yielded a healing efficiency of nearly 50%, and those healed at 80 $^{\circ}\text{C}$ had an average healing efficiency of 66%, with a maximum over 80%, corresponding to an increase of about a factor of 1.6.

4. Conclusions

We have shown that significant improvements in healing performance are achieved in epoxy samples with injected healing agent by incorporating SMA wires that bridge the fracture plane. During the self-healing process, the SMA wires can be used to decrease the crack volume, thus increasing the fill factor (DCPD volume divided by crack volume). The increased fill factor allows better healing performance with low amounts of healing agent. A fill factor of at least unity is needed to reach a maximum healed performance. The healed peak fracture loads were increased from 38 to 60 N on average when three SMA wires were embedded orthogonal to the crack plane of TDCB fracture samples and activated by resistive heating to 80 $^{\circ}\text{C}$ for 30 min following the virgin fracture event. This corresponds to an increase in healing efficiency from 49 to 77% with SMA wires. Furthermore, samples containing SMA wires and injected with only 1 μL of DCPD show healing efficiencies of around 50%.

In summary, the improvements in healing performance are due to two mechanisms. Firstly, the total crack volume that must be repaired is reduced upon SMA wire activation by closure of the crack faces in response to the closure forces exerted by the wires bridging the crack plane. Secondly, localized heating of the healing agent during activation leads to an increase in the degree of cure of the polymerized healing agent and improved mechanical and adhesive properties.

5. Experimental

For all tests, the matrix was EPON 828 resin (Shell Chemicals) cured with diethylenetriamine (DETA; Sigma-Aldrich), mixed in a 100:12 mass ratio. The SMA wires (Furukawa Electric, Tokyo) are 150 μm diameter, with a Ni/Ti/Cu composition 44.86:45.08:10.06. The transformation temperatures of the SMA wires were determined by differential scanning calorimetry and are shown in Table 2.

The self-healing properties were investigated using TDCB samples (Fig. 11). This geometry was developed by Mostovoy et al. [16], and provides a measurement of the fracture toughness that is independent of the initial crack length, i.e.,

$$K_{IC} = \alpha P_C \quad (3)$$

where P_C is the critical fracture load and $\alpha = 11.2 \times 10^3 \text{ m}^{-3/2}$, for this geometry [2].

Three SMA wires were each tensioned with a 50 g mass and embedded at the mid-plane of the sample, perpendicular to the crack direction (Fig. 11). Grubbs' first generation catalyst (Sigma-Aldrich) was recrystallized via a non-solvent addition method [17] and wax-encapsulated for protection to form 10 wt% Grubbs' catalyst in wax microspheres [3]. The microspheres were embedded in the sample in a 5 wt% concentration. In order to minimize costs, the microspheres were localized around the crack plane region [10]. The resin was degassed, cured in silicone rubber moulds for 24 h at room temperature, and post-cured at 35 °C for a further 24 h. After post-curing, a sharp pre-crack was made by tapping a razor blade into the molded starter-notch.

The TDCB samples were mounted in a load frame with two pins, and loaded in tension at a constant displacement rate of 5 $\mu\text{m s}^{-1}$. At failure, a crack propagated horizontally along the side-grooves, along the full length of the specimen, fracturing the sample into two halves. The SMA wires have a tensile strength of 1.34 GPa, and a maximum elongation of 13% before failure, so the wires remained intact when the sample failed. The peak load at failure was recorded, from which the virgin fracture toughness was calculated (Eq. 3).

The two sample halves were then removed from the load frame. The SMA wires were mechanically clamped at both locations where they exit the matrix. This eliminated any influence of the quality of the SMA interfacial bonding on the present measurements. For the measurements reported here, the DCPD was manually injected into the crack using a precision syringe. These injected TDCB samples produce equivalent performance as microcapsule samples, for the same amount of healing agent delivered [10]. The two halves were then brought back into contact, either by activating the SMA wires or else manually (for samples without SMA wires), and allowed to heal over a 24 h period. The SMA clamps were then removed, the SMA wires themselves carefully debonded and removed from the matrix by hand, and the samples re-tested to failure under the same conditions as for the virgin material, and the healed peak load and fracture toughness recorded.

The finish transformation temperature upon heating of an unconstrained wire is 65.6 °C (Table 2). Figure 12 shows the recovery stress exerted by a single fully constrained SMA wire versus activation temperature. The recovery stress continues to rise above the temperature of 65.6 °C because the wire is constrained at both ends

Table 2. SMA wires used for self-healing study.

Composition (Ni/Ti/Cu)	44.86:45.08:10.06
Diameter	150 μm
$T_{M,s}$	53.6 °C
$T_{M,f}$	47.1 °C
$T_{A,s}$	59.8 °C
$T_{A,f}$	65.6 °C

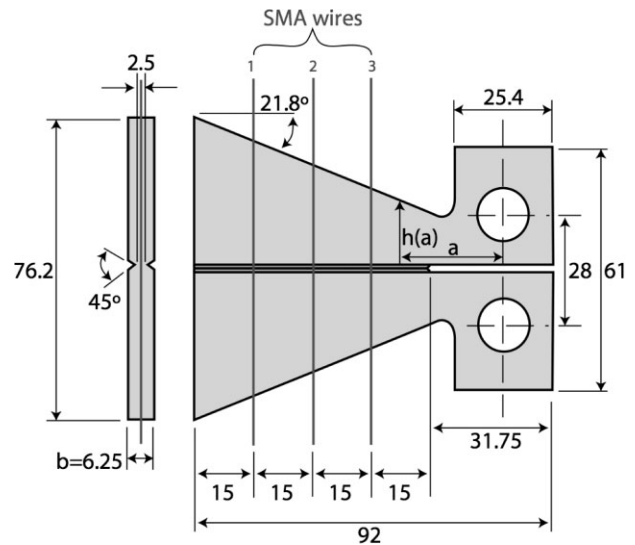


Figure 11. TDCB geometry of the test samples. Samples were prepared both without SMA wires and with three SMA wires perpendicular to the crack plane, spaced uniformly. The distance between the loading axis and the crack tip is a . All units in mm.

and so is not free to fully transform. An SMA wire activation temperature of 80 °C was selected, which generates a recovery stress of 240 MPa, yet remains sufficiently below the deactivation temperature in air of 140 °C of the embedded catalyst [17].

Heating was achieved by passing a current through the wire. To determine the SMA wire temperature in the test sample as a function of current, a sample was made in which a small thermocouple was located on each wire at the crack plane. Current was passed through the wires and the temperature monitored with time. Thermal equilibrium was achieved after about 10 min, and a current of 0.5 A per wire was sufficient to raise the wire temperature to 80 °C. The resistivity of a single SMA wire at 80 °C is 100 $\mu\Omega \text{ cm}$, corresponding to a resistance of 0.56 $\Omega \text{ cm}^{-1}$. So, at 0.5 A current, a power of about 0.14 W cm^{-1} of wire is dissipated. Typically, the current of 0.5 A per wire was maintained for half an hour after the initial fracture test, corresponding closely with the room temperature gel time of the DCPD. The sample was then

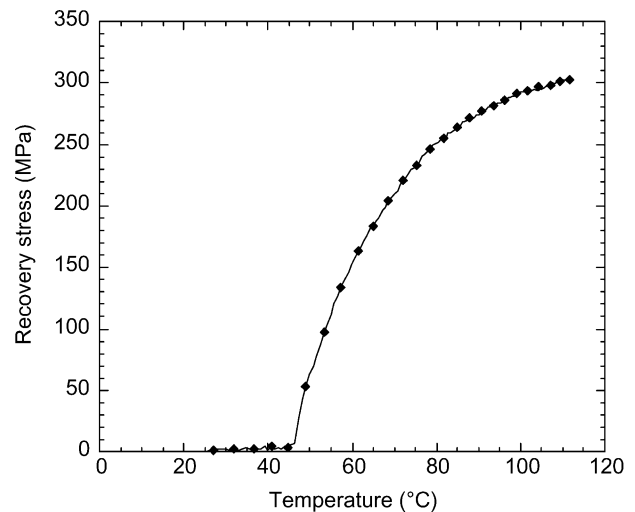


Figure 12. Recovery stress generated by a constrained SMA wire that is prestrained by 0%.

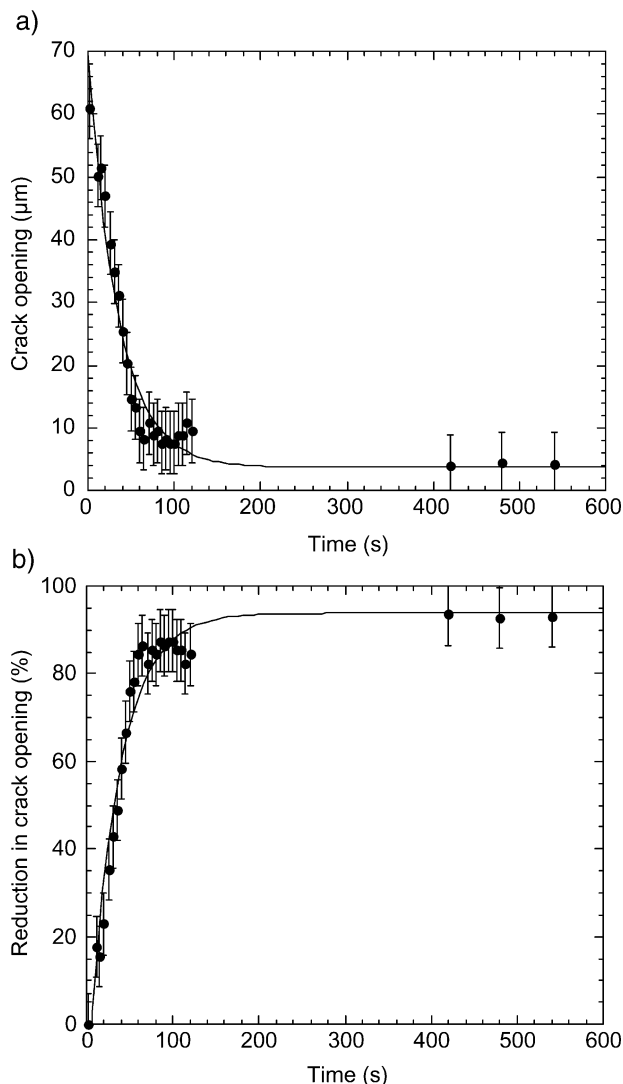


Figure 13. a) Crack opening versus SMA activation time and b) percent reduction in crack opening versus SMA activation time; 0.5 A current per wire.

allowed to heal at room temperature for 24 h. Figure 13 shows a typical measurement of the crack opening with SMA activation time, and the corresponding reduction in crack opening, respectively. A large

reduction of crack opening (~ 10) is achieved within approximately 60 s.

The self-healing performance of a material can be quantified by the healing efficiency [2]:

$$\eta = \frac{K_{IC_H}}{K_{IC_V}} = \frac{P_{C_H}}{P_{C_V}} \quad (4)$$

where K_{IC_V} and K_{IC_H} are the virgin and healed fracture toughness, respectively, and P_{C_V} and P_{C_H} are the virgin and healed peak loads at fracture, respectively. However, the virgin fracture toughness depends on microcapsule size and loading, and so η is a more difficult variable with which to interpret pure healing performance. Following the method used by Rule et al. [10], in this paper we compare healed peak loads to evaluate healing performance. However, average virgin peak load values are provided in Table 1 so that the healing efficiencies can be readily calculated.

Received: October 22, 2007

Revised: March 7, 2008

- [1] S. R. White, N. R. Sottos, P. H. Guebelle, J. S. Moore, M. R. Kessler, S. R. Sriram, E. N. Brown, S. Viswanathan, *Nature* **2001**, *409*, 794.
- [2] E. N. Brown, N. R. Sottos, S. R. White, *Exp. Mech.* **2002**, *42*, 372.
- [3] J. D. Rule, E. N. Brown, N. R. Sottos, S. R. White, J. S. Moore, *Adv. Mater.* **2005**, *17*, 205.
- [4] T. Yin, M. Z. Rong, M. Q. Zhang, G. C. Yang, *Compos. Sci. Technol.* **2007**, *67*, 201.
- [5] E. N. Brown, S. R. White, N. R. Sottos, *J. Mater. Sci.* **2004**, *39*, 1703.
- [6] J. W. C. Pang, I. P. Bond, *Compos. Sci. Technol.* **2005**, *65*, 1791.
- [7] R. S. Trask, I. P. Bond, *Smart Mater. Struct.* **2006**, *15*, 704.
- [8] R. S. Trask, G. J. Williams, I. P. Bond, *J. R. Soc. Interface* **2007**, *4*, 363.
- [9] K. Toohey, J. A. Lewis, J. S. Moore, S. R. White, N. R. Sottos, *Nat. Mater.* **2007**, *6*, 581.
- [10] J. D. Rule, S. R. White, N. R. Sottos, *Polymer* **2007**, *48*, 3520.
- [11] Z. G. Wei, R. Sandstrom, S. Miyazaki, *J. Mater. Sci.* **1983**, *33*, 3763.
- [12] J. Schrooten, V. Michaud, J. Parthenios, G. Psarras, C. Galiotis, R. Gotthardt, J. A. Månson, J. Van Humbeeck, *Mater. Trans, JIM* **2002**, *43*, 961.
- [13] K. A. Tsoi, J. Schrooten, R. Stalmans, *Mater. Sci. Eng, A* **2004**, *368*, 286.
- [14] C. A. Rogers, C. Liang, S. Li, Proceedings of *AIAA/ASME/ASCE/AMS/ASC 32nd Structures, Structural Dynamics and Materials Conference*, Baltimore **1991**, p. 1190.
- [15] M. R. Kessler, N. R. Sottos, S. R. White, *Compos. Part A* **2003**, *34*, 743.
- [16] S. Mostovoy, P. B. Crosley, E. J. Ripling, *J. Mater.* **1967**, *2*, 661.
- [17] A. S. Jones, J. D. Rule, J. S. Moore, S. R. White, N. R. Sottos, *Chem. Mater.* **2006**, *18*, 1312.